RAMAN–LIDAR DETECTION RANGE FOR CONTAMINATING GASEOUS SPECIES IN THE UV SOLAR BLIND REGION

Yu.F. Arshinov, S.M. Bobrovnikov, A.G. Popov, D.I. Shelefontyuk, and V.K. Shumskii

Institute of Atmospheric Optics,
Siberian Branch of the Russian Academy of Sciences, Tomsk
Received March 28, 1994

In this paper we present analysis of a Raman lidar for detecting gaseous pollutions of the atmosphere using UV sounding radiation. It is shown in the paper that a strong spectral dependence of the detection range occurs in the solar blind region. It is also shown that optimal wavelengths of sounding radiation can be found in the UV region that are more efficient for use to detect air pollution.

Necessity of making day and night observations of the atmosphere important for many meteorological and atmospheric optics studies imposes much more strict requirements on optical techniques and instrumentation for measuring atmospheric parameters. All lidar techniques are among such optical methods. Any lidar sensing technique suffers, to a considerable or lesser degree, from the optical noise, basically caused by the background solar radiation. It is obvious that suppression of optical noise due to scattering of solar radiation in the atmosphere is the main problem when performing day–time lidar observations. As to the lidar itself, as a laser radar device, it is easy enough to separate out its main characteristics that determine the noise protection of the whole lidar system. These parameters are

1. energy of a sounding radiation pulse,
2. mean power of sounding radiation,
3. field–of–view angle of optical receiving system,
4. width of the optical receiver pass band,
5. width of the photodetector pass band.

Of course, each of these characteristic makes its particular contribution to the formation of the resulting signal–to–noise ratio. Thus, for example, energy of a sounding radiation pulse can be restricted either because of technological conditions or due to eye safety limitations. The field–of–view angle of a receiver is usually limited, from below, by the least aberrations circle or by the turbulent blurring of a narrow laser beam.

It is quite clear that it is senseless to make a receiver's pass band narrower than the spectrum of received radiation. Ideally, the transmission function of a receiving optical system should coincide with the spectrum of received radiation.

Sometimes a proper choice of lidar parameters, in accordance with the requirements of day–time operation, could enable one to reach practically significant range of day–time operation. This is especially true in relation to the elastic–backscatter–based lidars like, for example, aerosol, differential absorption, and correlation lidars. It is obvious that the potentialities of such lidars are much higher at night. Most general approach to estimation of lidar potentialities that accounts for many different factors was proposed by B.V. Kaul' in Ref. 1. Using this approach it is possible to estimate performance parameters of a lidar system including its ability of operating during day time.

However, in the case of lidar systems which use weaker optical effects, compared to aerosol backscatter, like, for example, Raman effect, even the best fitted parameters of a lidar system cannot provide its day–time operation.

Sometimes the approach based on use of sounding radiation in the so–called solar blind spectral region is considered as the only possible and an obvious solution to this problem of day–time lidar operation. The matter is that solar radiation in this spectral region is entirely absorbed by ozone molecules in the stratospheric ozone layer. As a result, in the troposphere we have purely night–time conditions in this spectral region. However, the atmospheric oxygen and the tropospheric ozone, in their turn, impose certain limitations on the operation of lidars in this spectral region.

In this connection it seems to be worth considering in more detail the main factors determining propagation of the UV radiation in the troposphere. As known[2] absorption of light in the UV spectral region is determined by the electronic transitions of such atmospheric constituents as O_2, O, N_2, N, and O_3. All these components play an important role in photochemical processes in the middle atmosphere while the absorption of radiation in the solar blind region (200 to 300 nm) is governed only by ozone and oxygen.

Ozone molecules have in this region a very strong absorption band (Hartley absorption band) which causes an essential attenuation of UV radiation even when the ozone content in the troposphere is as low as its natural background. The molecular oxygen essentially prevents propagation of light at wavelengths shorter than 240 nm due to absorption within Herzberg continuum which, at 200 nm wavelengths, comes into the Schumann–Runge continuum. The strength of light absorption in this spectral region excludes any possibility of using sounding radiation at wavelengths shorter than 200 nm in the atmosphere.

In addition to the strong absorption of light, Rayleigh molecular scattering also essentially contributes into the total extinction of radiation by the atmosphere in the short–wave portion of the UV spectral region.

Figure 1 presents spectral behavior of the main factors causing the extinction of radiation by the atmosphere in the spectral region from 200 to 300 nm. The curves plotted in this figure have been calculated using experimental data on the absorption cross sections of O_2 and O_3 molecules and the molecular scattering cross section.[4] In calculations we took the concentrations of ozone and oxygen to be 40 ppb and 21% by volume. As is seen from Fig. 1, the spectral behavior of the total extinction coefficient (curve *4*) in this spectral region has certain peculiarities which allow us to isolate three different spectral portions in this region.

The first portion from 200 to 250 nm is characterized by a rapid fall off of the extinction from approximately 5.8 down to about 1.4 km^{-1}. It is obvious that use of this

0235-6880/94/08 609-03 $02.00

spectral region for lidar sensing of the atmosphere is too problematic, first because of huge energy losses and second because of difficulties that can appear due to large difference between the extinction coefficients at close wavelengths.

In the second portion from 250 to 265 nm the spectral behavior of the extinction can be neglected in many cases even if the ozone content of the atmosphere varies.

The basic feature of the spectral behavior of the tropospheric extinction in the third portion of this solar blind region is a monotonic and smooth fall off of the extinction coefficient almost down to the level of extinction due to molecular scattering. The curve presenting in this figure the spectral behavior of the total extinction coefficient of the troposphere bears quite obvious information useful for estimating potentialities of lidar systems operating in the solar blind region.

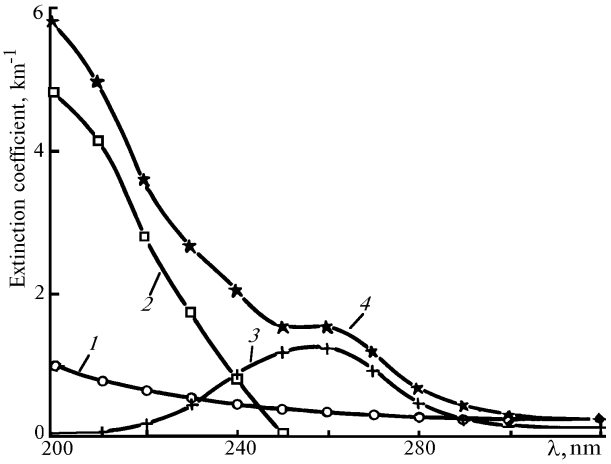

FIG. 1. Spectral behavior of the extinction coefficients due to the main radiation attenuation processes in the UV region. 1 – molecular scattering, 2 – absorption in the Herzberg continuum of molecular oxygen (n_{O_2} = 21%), 3 – absorption by ozone (n_{O_3} = 40 ppb) in the Hartley absorption band, 4 – total extinction coefficient.

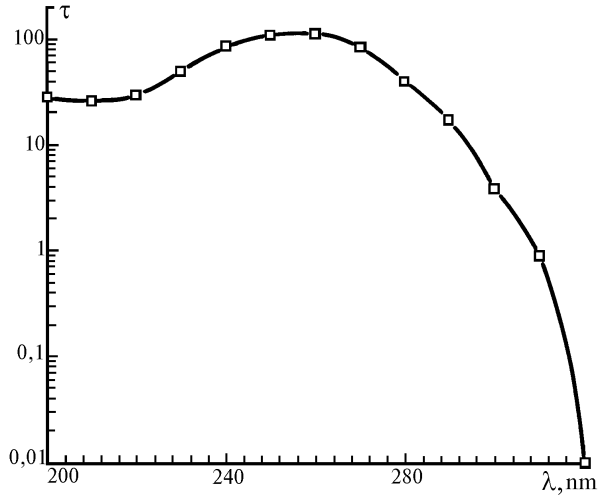

FIG. 2. Optical thickness, τ, of the atmospheric column calculated with the account for absorption by molecular oxygen and stratospheric ozone (the ozone column density was taken 0.4 cm*).*

Let us now consider the solar blind region in more detail. As was mentioned above, the stratospheric ozone prevents penetration of the UV solar radiation to the Earth's surface thus providing, in a certain wavelength range, night–time conditions for operation of ground–based optical systems. It is evident that absorption bands of molecular oxygen also contribute into the extinction of solar radiation in the short–wave spectral region. Using data on column densities of the ozone and oxygen and on the absorption cross sections of O_3 molecules in Hartley band and O_2 molecules within Herzberg continuum one can calculate optical thickness of the atmospheric column in the spectral region under study. Results of such calculations are shown in Fig. 2. As is seen from the figure, the optical thickness, τ, of the vertical atmospheric column at the wavelengths shorter than 280 nm reaches very big values. Thus at maximum near 260–nm wavelength it exceeds 100.

In order to estimate the level of atmospheric attenuation of solar radiation in this spectral region, it seems to be more convenient to plot the spectral behavior of the atmospheric transmission in this same spectral region ($T(\lambda) = \exp(-\tau(\lambda))$). Here and below we consider the transmission of a vertical column of the atmosphere, that means for negligibly small zenith angles of the Sun what is not realistic at midlatitudes. Obviously, at larger zenith angles of the Sun the attenuation of radiation by the atmospheric column is much stronger. So, the spectral behavior of the transmission of a vertical atmospheric column is shown in Fig. 3. The dashed horizontal lines in the figure show the levels of extinction corresponding to day– and night–time conditions. Night–time conditions are defined according to criterion of 10^{-8} atmospheric transmission for solar radiation.[5] According to this criterion one can determine the wavelength of red boundary of solar blind region. The spectral region to the left from this wavelength corresponds to night–time conditions while to the right from it there are twilight and day. Spectral region between the wavelengths λ_n = 290 nm and λ_d = 320 nm could be called as "ever twilight" sky.

Thus, the spectral region between the wavelengths λ = 200 m and λ = 290 nm can be defined as a solar blind region where the conditions of illumination by solar radiation correspond to night–time. The short–wave boundary of this region is chosen at 200 nm wavelength because of a disastrous increase of absorption within Schumann–Runge continuum at shorter wavelengths.

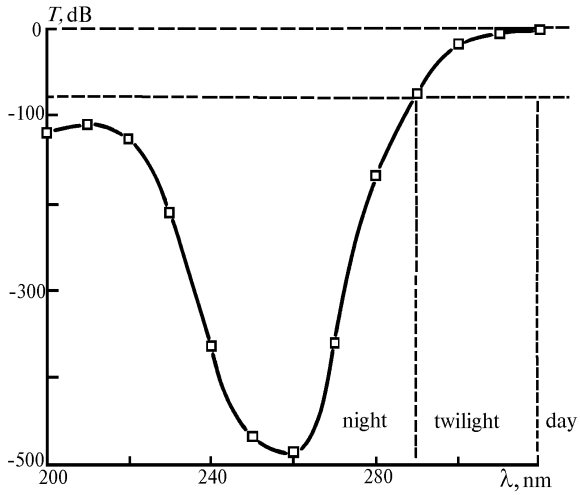

FIG. 3. Extinction of radiation by the vertical column of the atmosphere. The lower dashed horizontal line shows the extinction level of 10^{-8}, that corresponds to night–time conditions.

As is seen from Fig. 3, the spectral behavior of extinction in this region is essentially nonuniform, but nevertheless the background from solar radiation in this portion of spectrum can be neglected in the majority of cases.

As noted above the molecular oxygen and ozone of the troposphere limit somewhat the freedom of using UV solar blind region, especially of its short–wave portion. In order to elucidate realistic potential of a particular lidar system to operate during day–time, it would be useful to conduct a numerical experiment. In doing this let us set the specifications of a lidar to be as follows.

Lidar Specifications

Diameter of a receiving aperture, m	0.5
Width of instrumental contour of a lidar spectrometer, cm^{-1}	8
Transmission of the receiving optical channel	0.1
Quantum efficiency of a photodetector	0.1
Field–of–view angle of the optical receiver, mrad	0.3
Mean power of sounding radiation, W	10
Measurement time, min	30
Spatial resolution, m	10

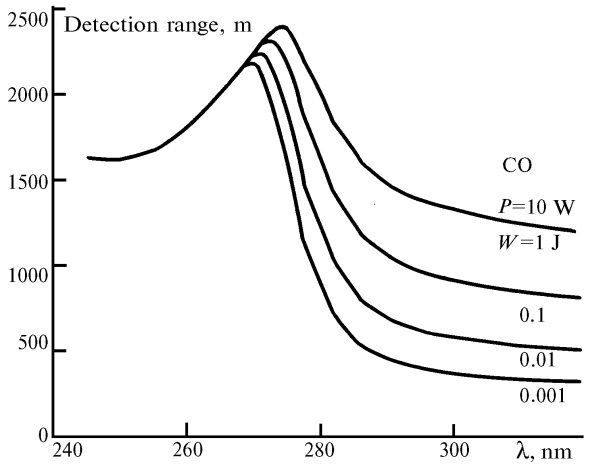

FIG. 4. Day–time detection range for carbon monoxide (n = 100 ppm) as a function of wavelength of sounding radiation, for different pulse energy W at a fixed mean power P = 10 W.

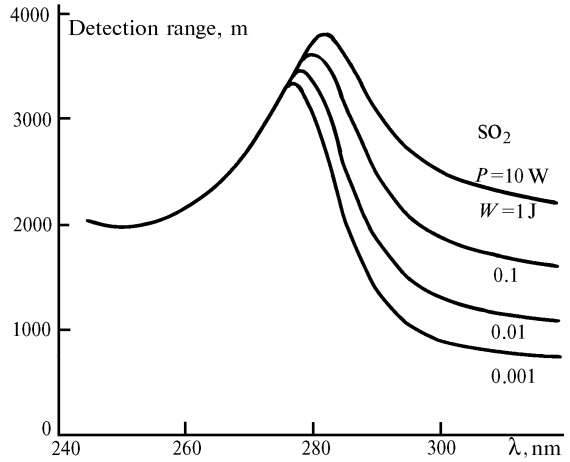

FIG. 5. Day–time detection range for sulfur dioxide (n = 100 ppm) as a function of wavelength of sounding radiation, for different pulse energy W at a fixed mean power P = 10 W.

Figures 4–6 show the results of numerical simulations on calculating spectral behaviors of the range at which some small amounts of the basic pollutants (carbon monoxide CO and sulfur dioxide SO_2) could be detected with a Raman lidar. The families of curves in Figs. 4 and 5 were calculated assuming constant mean power of a pulsed sounding radiation, while changing energy per pulse (figures at the curves). For the detection criterion we took the condition of storing 10 signal photocounts. It is obvious that curves depicted in Figs. 4 and 5 are very similar. Such spectral behaviors of the detection range could be calculated for any other gas provided that its Raman frequency shift and cross section are known. It is well seen from these figures that in the twilight portion of the solar blind region, where solar background is suppressed only partially, the detection range strongly depends on the pulse energy of sounding radiation. At the same time, there is some wavelength λ_n, to the left from which all curves calculated for a particular gas coincide. That means that in this region the mean power of sounding radiation is the decisive factor determining the sounding range of a lidar. In other words, just this wavelength determines the red boundary of a solar blind region for detection of a particular gaseous specie calculated in accordance with the above chosen detection criterion. The differences in the detection range and the positions of the red boundary for CO and SO_2 are well seen from Figs. 4–6 what is explained by different Raman shifts and cross sections of the Raman scattering process for these two molecules.

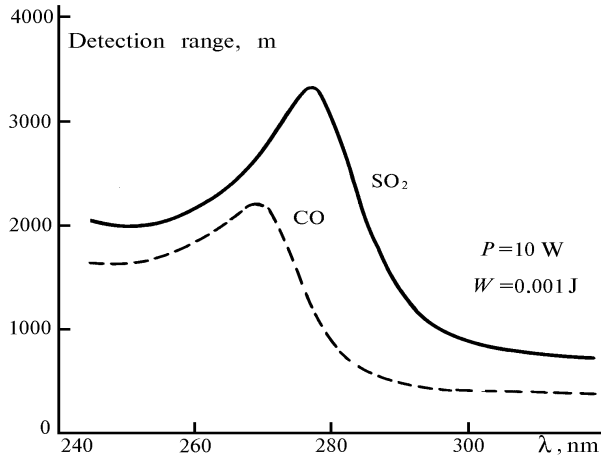

FIG. 6. Comparison of spectral behaviors of the detection range for CO and SO_2 molecules whose Raman frequency shifts are 2145 cm^{-1} (CO) and 1151 cm^{-1} (SO_2), the concentration of both gases being 100 ppm.

The above analysis of the use of solar blind region for lidar sensing of air pollution from the standpoint of feasibility of day– and night–time operation, allows one to conclude that the concept of solar blind region, in this case, is in fact relative. Thus the position of its red boundary depends on a particular Raman shift of a specie. It is also evident from this analysis that it is advisable to use sounding radiation whose wavelength is in the close vicinity of a red boundary since in this case optical losses due to light absorption by tropospheric ozone would be minimum (see the positions of maxima of the spectral curves in Figs. 4–6). It is also obvious that there is no optimum wavelength of sounding radiation for detecting several gases simultaneously. In the case of a set of gases to be detected simultaneously, the gas whose Raman shift in the spectrum of scattered radiation is the largest will determine the choice of a proper wavelength of sounding radiation.

In conclusion it can be said that despite of many inevitable drawbacks appearing in the case of sounding air pollution in the solar blind region it is worth using this region for lidar sensing since, for example, the optical losses are compensated for by the increase of Raman cross sections.

This paper presents only one step in the development of solar blind lidar facilities.

ACKNOWLEDGMENTS

Finally, we should like to acknowledge Special Foundation for Supporting Young Gifted Scientists which partially funded this work.

REFERENCES

1. B.V. Kaul', Atm. Opt. **2**, No. 2, 166–169 (1989).
2. G.P. Gushchin and N.N. Vinogradova, *Total Ozone of the Atmosphere* (Gidrometeoizdat, Leningrad, 1983), 238 pp.
3. *Handbook "Atmosphere"* (Gidrometeoizdat, Leningrad, 1991), 509 pp.
4. S.P. Perov and A.Kh. Khrgian, *Modern Problems of the Atmospheric Ozone* (Gidrometeoizdat, Leningrad, 1980), 287 pp.
5. V.E. Zuev and M.V. Kabanov, *Current Problems of the Atmospheric Optics: Optics of Atmospheric Aerosol* (Gidrometeoizdat, Leningrad, 1987), Vol. 4, 254 pp.